· Article · Advances in Polar Science

doi: 10.3724/SP.J.1085.2011.00081 June 2011 Vol.22 No.2: 81–91

Shock effects and the classification of H-chondrites from the Grove Mountains, East Antarctica: Implications for the shock history of H-chondrite parent bodies

WANG BaoHua[1,2], MIAO BingKui[1,2*], WANG Jiang [1,2] & ZHANG Jian[1,2]

[1] Key Laboratory of Geological Engineering Centre of Guangxi Province, Guilin University of Technology, Guilin 541004, China;
[2] College of Earth Sciences, Guilin University of Technology, Guilin 541004, China

Received March 1, 2011; accepted May 4, 2011

Abstract The shock metamorphism of 47 H group chondrites (H-chondrites) from the Grove Mountains including undulatory extinction, planar fractures, mosaic extinction, shock veins and pockets, and dendritic eutectic metal-sulfide, is observed through optical microscope. The textures and assemblages of shock veins in these H-chondrites are examined by the scanning electron microscope. Based on observations of the above shock effects, the shock stages of the 47 H-chondrites are classified into S1(5), S2(19), S3(14), S4(8) and S5(1). Of these H-chondrites, GRV 022469 has the highest(S5) shock stage. The comparison of shock stages in these H-chondrites with L group chondrites(L-chondrites) indicates that the shock metamorphism of H-chondrites is relatively low (except for GRV 022469, they are all lower than S5). A scenario for the history of the H-chondrite parent body is proposed that suggests the duration of the shock events in the H-chondrite parent bodies was much shorter than those in L-chondrite parent bodies. Also, the pressure may have been released more quickly, and consequently, the high-pressure phases should be easily preserved. However, the parent bodies of the H-chondrites may have been exposed to high temperatures for a longer time after the shock event, so the high-pressure phases formed by solid transformation might have retro-metamorphosed to low-pressure ones; its peak pressure is estimated to be less than 15 GPa. Wadsleyite was found in a shock vein in GRV022469, as confirmed by the Raman spectrometer. Petrological and mineralogical characteristics support the idea that the wadsleyite was formed by solid-state transformation.

Keywords Ordinary chondrite, Grove Mountains, H-chondrite, shock stage, Wadsleyite

Citation: Wang B H, Miao B K, Wang J, et al. Shock effects and the classification of H-chondrites from the Grove Mountains, East Antarctica: Implications for the shock history of H-chondrite parent bodies. Adv Polar Sci, 2011, 22: 81—91, doi: 10.3724/SP.J.1085.2011.00081

0 Introduction

The shock metamorphism of meteorites is one of the most important aspects of meteorite research. The effects caused by shock events during the formation and evolution of planets can reveal important information on the conditions and environments of impacts and the mechanisms of planet formation, providing insight into the impact history of the solar system. The process of shock wave spreading causes the inhomogeneous distribution of temperatures and pressures in the meteorite parent body, variation in minerals (e.g.,olivine, pyroxene and plagioclase) and/or assemblages, and changes in their compositions and textures. These changes in minerals caused by shock effects include irregular and planar fractures, undulatory and mosaic extinction, shock veins, isotropization of plagioclase (maskelynite) and high-pressure phase transformation[1–3].

Based on these shock metamorphic effects, the shock metamorphism of meteorites can be classified into different stages (e.g., S1-S6 by Stöffler, 1991)[4]. Previous studies of shock metamorphism in ordinary chondrites have primarily addressed L-chondrites[5–8]. The study of shock metamorphism in H-chondrites is limited, and only three H-chondrites have been reported to exhibit high shock stages associated with high pressure phases[9–11]. To further

*Corresponding author (miaobk@glite.edu.cn)
Wang Baohua, male, Master degree, assistant professor, cosmochemistry

investigate shock metamorphism in H-chondrites, and find more H-chondrite samples with high shock stages, we carry out a systematic examination of shock metamorphism in 47 H-chondrite samples from the Grove Mountains where is an inland ice sheet with 64 nunataks in East Antarctica.

The shock stages of the 47 H-chondrites are classified according to Stöffler's criteria for the shock stages of ordinary chondrites. Based on the analysis of their shock effects, the mechanics and history of shock metamorphism in the parent body of the H-chondrites are discussed further.

1 Samples and experiments

The samples for this work are 47 H-chondrites from the Grove Mountains, East Antarctica. Shock metamorphic effects, including irregular and planar fractures, undulatory and mosaic extinction, maskelynite and shock-induced veins, are observed and identified under an optical microscope (Leica DMEP). The textures and compositions of minerals in shock-induced veins and/or pockets are examined by Scanning Electron Microscope (JEOL JSM-6460 LV) equipped with an X-ray energy spectrometer (Genesis EDAX). The accelerating voltage is 20 kV. The fine-grained minerals and assemblages in the shock-induced veins are identified by micro-Raman (Reinshaw Invia Reflex) with an Ar^+ laser in the Institute of Geochemisty，Chinese Academy of Sciences. The wavelength is 514.5 nm. The laser spot is 1 μm across, and the peak resolution is 2 cm^{-1}.

2 Shock metamorphic effects

2.1 Fracture, undulatory extinction, and mosaic extinction

As shown in Table 1, undulatory extinction is observed in the main minerals (i.e., olivine and pyroxene) in the host rock, and also in some olivine grains entrained in the shock veins from all samples with shock stages higher than S1. The minerals with undulatory extinction usually have developed irregular and/or planar fractures (Figure 1A). Olivine grains have fractures with various degrees (Figure 1B). In all these samples, olivine has irregular fractures with various densities. However, planar fractures occur in the meteorites with higher shock stages. Planar fractures usually extend along the special crystallographic direction (Figure 1C). The common occurrence of planar fractures indicates a shock stage of S3. In addition, the chromite-plagioclase assemblage is considered to be an indicator of shock stage S3 in ordinary chondrites[2].

Of the 47 H-chondrites, nine are found to have olivine grains in the shock veins showing mosaic extinction. However, their occurrences differ. Some are in the middle of shock veins, whereas others are on both sides of shock veins, close to the boundaries. Under the cross-polarized light of an optical microscope, the mosaic extinction of olivine grains exhibits a series of optical extinction differences of ~5° in a local area of less than 0.3 mm^2. Mosaic extinction in the H-chondrites mostly occurs in the rims of single olivine grains, with individual mosaic fragments that are about 10 μm across (Figure 1D). The presence of mosaic extinction indicates that these H-chondrites have S4 shock stages.

Table 1 Shock metamorphic features and shock degrees of 47 H-Chondrites from the Grove Mountains

Meteorites	Type	Shock stages	OE	UE	PF	ME	CPA	SD	IT	MTD
GRV021984	H6	S1	▲							
GRV022329	H5	S1	▲							
GRV022967	H4	S1	▲							
GRV022986	H5	S1	▲							
GRV023106	H5	S1	▲							
GRV020220	H4	S2		▲						
GRV020228	H4	S2		▲			▲			
GRV021554	H4	S2		▲						▲
GRV021592	H4	S2		▲					▲	
GRV021720	H4	S2		▲						
GRV021824	H4	S2		▲						

(To be continued on the next page)

（continued）

Meteorites	Type	Shock stages	OE	UE	PF	ME	CPA	SD	IT	MTD
GRV021831	H5	S2		▲					▲	
GRV021895	H4	S2		▲	▲				▲	
GRV022429	H4	S2		▲					▲	
GRV022583	H5	S2		▲				▲	▲	
GRV023037	H6	S2		▲						
GRV023129	H5	S2		▲						
GRV023310	H6	S2		▲						
GRV052204	H5	S2		▲			▲			
GRV052308	H4	S2		▲						
GRV052346	H3	S2		▲						
GRV052658	H4	S2		▲						
GRV053363	H5	S2		▲						
GRV054472	H3	S2		▲						
GRV020219	H4	S3		▲	▲				▲	
GRV020266	H4	S3		▲	▲		▲			▲
GRV021205	H5	S3		▲	▲					
GRV021744	H4	S3		▲	▲					
GRV021827	H5	S3		▲	▲				▲	
GRV021913	H4	S3		▲	▲		▲			
GRV021964	H5	S3		▲	▲		▲			
GRV022468	H4	S3		▲	▲					
GRV022552	H3	S3		▲	▲		▲			
GRV022800	H4	S3		▲	▲					
GRV022955	H4	S3		▲	▲				▲	
GRV023047	H6	S3		▲	▲		▲	▲		
GRV050411	H4	S3		▲	▲					
GRV051951	H4	S3		▲	▲					
GRV020277	H4	S4		▲		▲			▲	
GRV021877	H5	S4		▲	▲	▲				▲
GRV021902	H4	S4		▲		▲	▲		▲	
GRV022641	H5	S4		▲		▲	▲	▲		▲
GRV022856	H5	S4		▲		▲				
GRV023127	H6	S4		▲		▲				
GRV023267	H5	S4		▲		▲		▲		
GRV053196	H5	S4		▲	▲	▲	▲			▲
GRV022469	H5	S5		▲		▲				▲

Notes: OE = optical extinction; UE = undulatory extinction; PF=Planar fracture; ME = Mosaic extinction; CPA = chromite-plagioclase assemblage; SD = silicate darkening; IT = irregular shaped troilite; MTD = dendritic eutectic texture metal-sulfide.

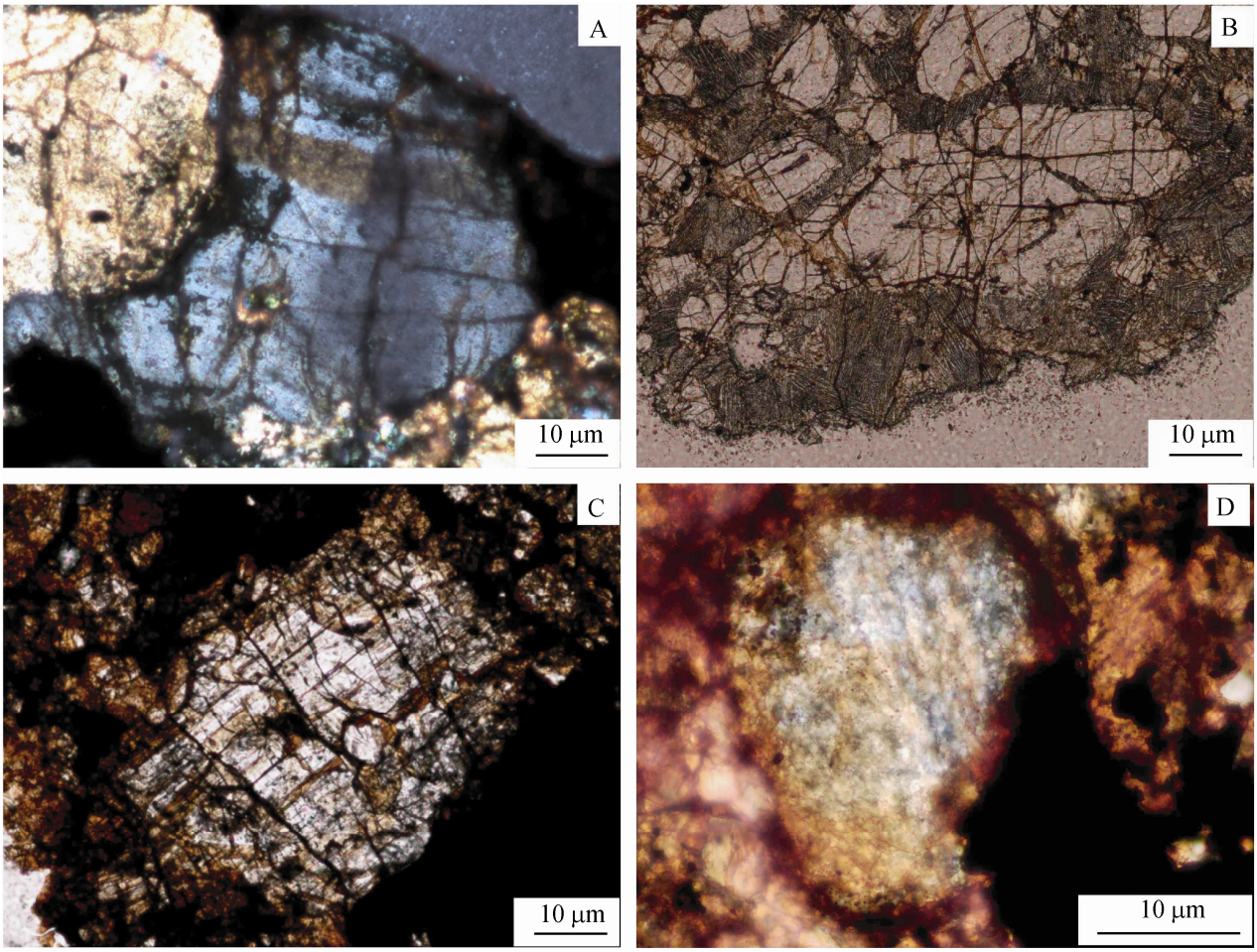

Figure 1 A. The grey olivine displays undulatory extinction in GRV 023037, cross-polarized light; B. GRV 022468, olivine in the center of photograph exhibits irregular fractures, plane-polarized light; C. GRV 021744, olivine in the center of photograph exhibits two sets of planar fractures nearly perpendicular to each other, plane-polarized light; D. olivine in the shock-induced melt vein of GRV 053196 displays mosaic extinction.

2.2 Chromite-plagioclase assemblages and maskelynite

The chromite-plagioclase assemblages observed in the meteorite samples mainly occur as pockets (10–20 μm in size) along fractures or at the boundaries of shock veins. In the chromite-plagioclase assemblages, euhedral or sub-idiomorphic chromite grains are embedded in an anhedral plagioclase matrix. The chromite grains are 0.5–10 μm in size and account for ~10% of the volume. Additionally, there is some irregular troilite and a minor amount of metal exhibiting a dendritic eutectic texture (<30 μm) around the assemblages (Figure 2).

Maskelynite shows complete extinction under the cross-polarized light of an optical microscope. The presence of maskelynite indicates an S5 shock stage, but no maskelynite grains are found in these H-chondrites. This is confirmed by Raman investigation.

2.3 Shock veins and the phase transformation of silicates

Shock melt veins and pockets are commonly observed in the chondrite samples with shock stages higher than S3. Ten of the H-chondrites were chosen for detailed examination. The shock veins in these H-chondrites can be classified as broad (≥200 μm wide) or thin (<200 μm wide)[12]. The widths of the shock veins are listed in Table 2, which shows that two meteorites are identified as belonging in the broad shock vein group. Two chondrite samples (GRV 053196 and GRV 022469) are chosen to compare the shock effects of the two groups in the following discussion.

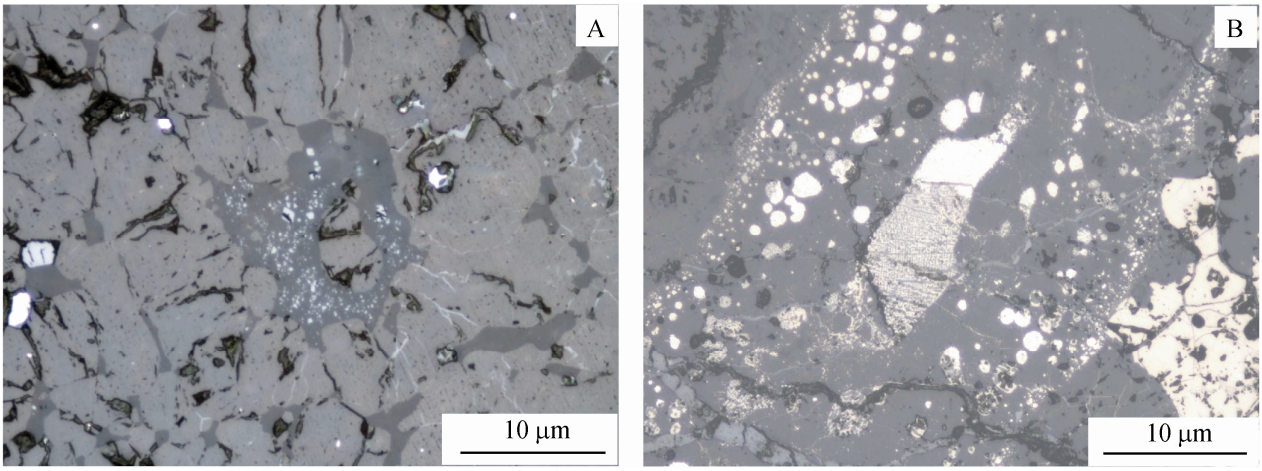

Figure 2 A. reflected-light image of GRV 022641 showing a chromite-plagioclase assemblage. The size of chromite is about 0.5 μm; B. metal-sulfide eutectic showing dendritic-like texture in a shock-induced melt vein of GRV 022469.

Table 2 Widths of shock-induced melt veins

Meteorite	Type	Shock stage	Width of shock vein /μm
GRV021592	H4	S2	65
GRV023047	H6	S2	25–50
GRV053363	H5	S2	30–200
GRV053196	H5	S3	65–185
GRV020266	H4	S3	50–150
GRV021877	H5	S4	100–200
GRV021902	H4	S4	250
GRV022856	H5	S4	35–65
GRV023267	H5	S4	85–200
GRV022469	H5	S5	250

Two shock veins cut across the thin section of GRV 053196, with one of the thin shock veins connecting with a shock melt pocket. The melt pocket is near the fusion crust and is 1.25 mm wide. The shock veins exhibit a porphyroclastic texture. The porphyroclasts consist of angular silicate fragments and round and/or irregular metal-sulfide grains. The metal and sulfide of the porphyroclasts in two shock veins usually have round boundaries and are 5–50 μm in size, but their interiors have two types: compact and dendritic eutectic (Figure 3). The silicate fragments of porphyroclasts, which are 5–25 μm in size, are olivine and low-Ca pyroxene. The matrix consists mainly of fine-grains of silicates and metal-sulfide, which are smaller than a few microns wide. EDS analyses show that the composition of olivine in the shock vein boundary is $Fa_{20.8}$, and the coexisting pyroxene has a composition of $Fs_{19.7}$. The FeO content of the silicates in the shock vein is slightly higher than those of the host silicates ($Fa_{18.2}$ for olivine and $Fs_{16.7}$ for pyroxene), but still remains within the range of the H group (Table 3).

The matrix of another shock vein in GRV 053196 is mainly composed of fine-grains of pyroxene and metal-oxide that are 1–2 μm wide. The metal and sulfides at the center of the veins occur as granular droplets and/or thin veinlets (20–70 μm wide). The fragments are mostly olivine and pyroxene, which are round and 10–30 μm across (Figure 3B). The FeO values of olivine (Fa_{22}) and pyroxene ($Fs_{24.9}$)

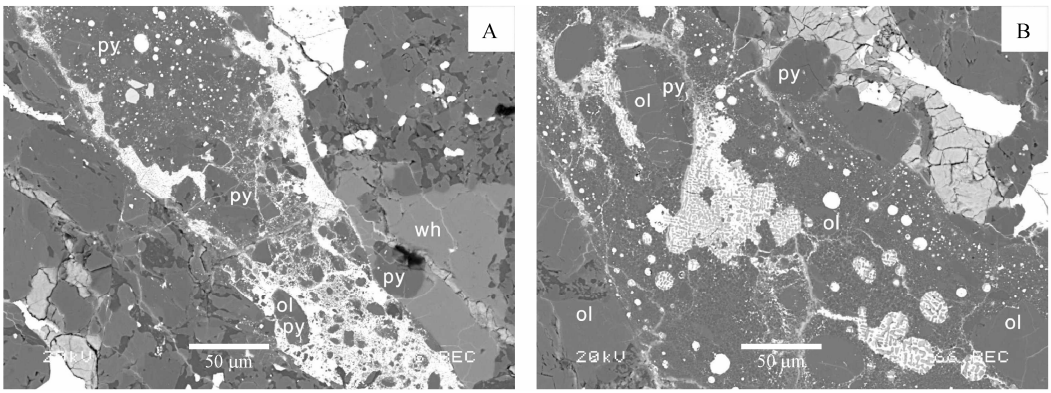

Figure 3 BSE images of two shock-induced melt veins in GRV 053196. A. Fragments of host chondrite fragments inside and outside the shock-induced melt vein; B. Silicate fragments and silicate, metal-sulfide matrix in the vein. ol-olivine; py-pyroxene; wh-whitlockite.

that are surrounded by eutectic metal and sulfide are higher than those in the host rock, and also beyond the H group range. No high-pressure phases are found in the Raman spectra analyses.

The mineral assemblages in the shock veins of the other seven H-chondrites are similar to those of GRV 053196. The matrix of shock veins is composed of fine-grained (< 5 μm) metal-oxide, olivine and pyroxene, whereas the coarse-grained (>10 μm) fragments surrounded by the matrix are olivine and pyroxene.

Table 3 EDAX results of minerals in shock-induced melt vein of GRV 053196（Mol %）

	Host olivine	Host pyroxene	Figure 3A olivine	Figure 3A pyroxene	Figure 3A pyroxene	Figure 3A pyroxene	Figure 3B olivine	Figure 3B pyroxene
O	59.2	60.1	57.1	59.6	59.2	59.8	57.1	60.4
Si	13.6	20.2	14	20	20.3	20.1	13.8	19.4
Al	0.02	0.04	0.04	b.d.	0.08	0.04	0.05	b.d.
Mg	21.7	15.7	22.2	15.7	15.8	15.7	21.8	14.3
Cr	b.d.	b.d.	b.d.	b.d.	0.02	b.d.	0.01	b.d.
Fe	4.82	3.19	5.85	3.9	3.65	3.56	6.15	4.92
Mn	0.13	0.15	0.13	0.15	0.16	0.17	0.15	0.1
Ni	b.d.	0.03	0.07	0.09	0.04	0.05	0.07	0.14
Ca	b.d.	0.18	0.03	0.17	0.29	0.21	0.03	0.63
Na	0.46	0.4	0.47	0.27	0.35	0.33	0.54	b.d.
K	b.d.	0.03	0.02	0.01	0.03	b.d.	0.05	0.08
P	b.d.	b.d.	b.d.	0.02	b.d.	b.d.	0.02	b.d.
S	0.05	0.02	0.2	0.08	0.06	0.04	0.34	0.15
Total	100	100	100	100	100	100	100	100
Fa	18.2		20.1				22	
En		82.3		79.4	80.1	80.7		72.0
Fs		16.7		19.7	18.5	18.3		24.9
Wo		1.0		0.9	1.5	1.1		3.2

Notes: Analyses shown here correspond to Figures 3A and 3B, b.d.- below detection limit.

GRV 022469 has the widest shock vein observed in this work. The vein has a generally porphyroclastic texture. The porphyroclasts are mainly metal-sulfide nodules and host silicate fragments, whereas the matrix consists of fine-grained (< 2 μm across) silicates. However, the grain sizes and mineral distribution vary from the center to side of the vein. On both sides of the shock vein, the metal-sulfide nodules are much smaller (~2μm wide) with a eutectic interior, whereas in the center the metal-sulfide nodules are much bigger (10–30 μm across) and have a eutectic texture. The coarse-grained mineral fragments are granular (20 μm wide) and consist mainly of olivine and pyroxene. The metal is kamacite and the sulfide is troilite. The fine-grained matrix mainly consists of metal oxide and pyroxene. The fragments embedded in the matrix are olivine and pyroxene, which are rounded and smooth (Figure 4A). The Fa value of olivine in the shock vein is nearly identical to that in the host rock olivine, and the Fs value of pyroxene fragment in the shock vein is also similar to that of the host rock pyroxene outside the shock vein.

Figure 4B shows a 2000-times enlarged BSE image of the center of the shock vein. The olivine fragments (15 μm across) embedded in the matrix are round. Using EDS measurements, points 1 and 3 (pyroxene) have higher Fs values than the average Fs value of the host rock pyroxene (Table 4). Similarly, the olivine inside the shock vein is more enriched in FeO than the olivine in the host rock outside the vein. However, its Fa content ($Fa_{20.4}$) is still in the range of the H group. Raman spectra analyses show that the matrix at the center of the GRV 022469 shock vein is composed of polycrystalline aggregates of fine-grained silicates.

The 712 cm^{-1} and 920 cm^{-1} peaks indicate that the aggregates contain wadsleyite(Figure 5), a high-pressure phase of olivine[5, 13–17]. The wadsleyite forms as a small round grain with a smooth surface surrounded by fine-grained (~1 μm across) pyroxene and metal oxides.

No high-pressure phases were found during the observation and analysis of shock veins in other meteorites in the study.

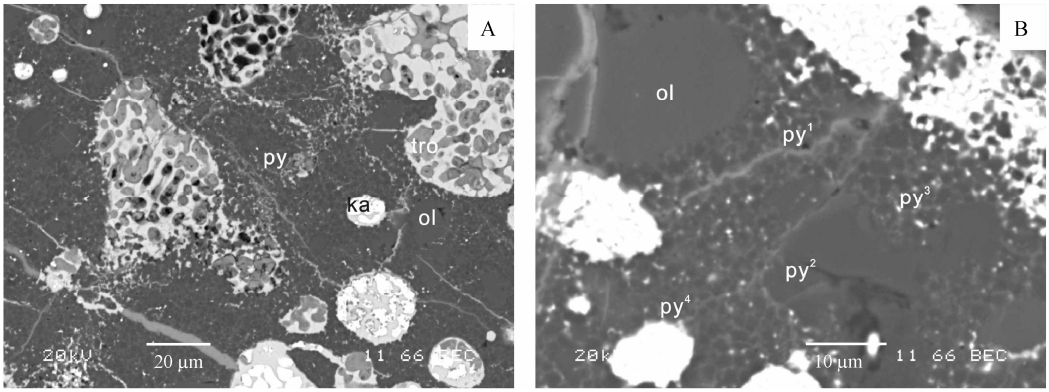

Figure 4 BSE images of a shock-induced melt vein in GRV 022469. A. The general texture of shock-induced melt vein; B. The mineral assemblage of fine-grained matrix in a shock-induced melt vein. ol-olivine; py-pyroxene; ka-kamacite; tro-troilite.

Table 4 EDS results of minerals in shock-induced melt veins in GRV 022469（Mol%）

	Figure 4A	Figure 4A	Figure 4A	Figure 4A	Figure 4B	Figure 4B	Figure 4B	Figure 4B	Figure 4B	Host	Host
	Kamacite	Troilite	Olivine	Pyroxene	Olivine	Pyroxene[1]	Pyroxene[2]	Pyroxene[3]	Pyroxene[4]	Olivine	Olivine
O	14.1	16.4	57.6	60.0	56.1	60.4	58.4	56.4	59.5	57.2	59.0
Si	b.d.	0.46	14.2	19.0	14.4	20	20.7	16.7	20.5	14.3	20.8
Al	b.d.	b.d.	b.d.	b.d.	0.03	b.d.	0.02	b.d.	b.d.	b.d.	0.04
Mg	0.29	0.83	22.6	15.8	22.9	13.3	16.2	13.8	14.7	22.7	16.1
Cr	b.d.	0.02	b.d.	0.15	0.02	0.09	b.d.	0.09	0.1	b.d.	0.02
Fe	77.6	38.8	4.82	3.35	5.86	4.75	3.89	8.99	4.02	5.06	3.11
Mn	b.d.	0.03	0.16	0.09	0.15	0.1	0.14	0.09	0.09	0.13	0.14
Ni	6.4	0.48	0.08	0.07	0.06	b.d.	0.03	0.19	b.d.	0.12	0.04
Ca	b.d.	0.03	0.03	0.76	0.03	1.12	0.25	1.01	0.82	b.d.	0.28
Na	0.54	0.4	0.43	b.d.	0.51	b.d.	0.34	b.d.	b.d.	0.49	0.36
K	0.05	0.05	0.03	0.05	0.02	0.09	0.02	0.1	0.07	0.02	0.05
P	b.d.	b.d.	b.d.	b.d.	0.03	b.d.	b.d.	b.d.	b.d.	b.d.	b.d.
S	1.02	42.5	0.05	0.81	0.08	0.11	0.07	2.64	0.21	0.08	0.07
Total	100	100	100	100	100	100	100	100	100	100	100
Fa			17.6		20.4					18.2	
En				79.3		69.4	79.6	58	75.2		82.6
Fs				16.8		24.8	19.2	37.8	20.6		16
Wo				3.8		5.8	1.2	4.2	4.2		1.4

Notes: these analyses correspond to Figures 3A and 3B, b.d.-below the detection limit.

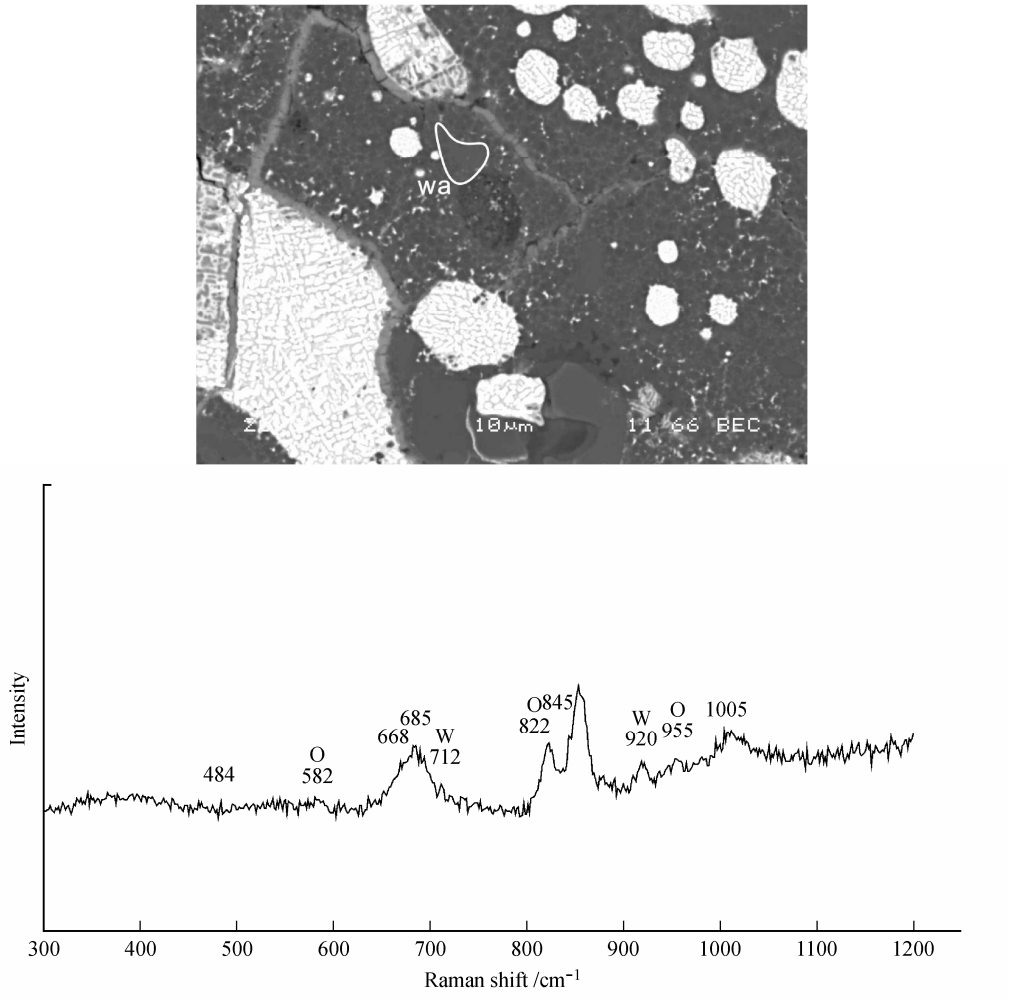

Figure 5 BSE image and Raman spectrum of olivine and wadsleyite polycrystalline aggregates from the shock-induced melt vein in GRV022469. Both 712 cm^{-1} and 920 cm^{-1} positions indicate the presence of wadsleyite. O- olivine, W- wadsleyite. The width of the BSE image is 120 μm.

2.4 Classification of shock stages

Based on Stöffler's (1991) criteria of shock stages for ordinary chondrites (i.e., extinction, fractures, melting, recrystallization and mineral assemblages of host silicates) combined with Feng's (2009) parameters for the S5 classification of the ordinary chondrites from the Grove Mountains[18], the shock stages of the 47 chondrites presented here are classified into: S1 (5), S2 (19), S3 (14), S4 (8) and S5 (1). The detailed results are listed in Table 1.

3 Discussion

3.1 Distribution of shock metamorphic stages for H-chondrites

Comparing the GRV H-chondrites in this work, with non-Antarctic H-chondrites in the Meteoritical Bulletin Database (MBD)* and the results of Stöffler(1991)[4] and Feng(2009)[18] (Table 5), we found the following features of shock metamorphism in H-chondrites.

(1) Except for one meteorite (S5) in this work, H-chondrites have lower shock stages, usually less than S4.

(2) Relatively speaking, H-chondrites from Grove Mountains have a greater proportion of higher shock stages than non- Antarctic H-chondrites, whereas the higher shock stages of non-Antarctic H-chondrites account for a lower proportion of 4% with S4.

(3) The shock stages of H-chondrites are concentrated at S2 to S3, which in total account for more than 70%.

(4) The L-chondrite parent body appears to have experienced higher shock metamorphism, since it has a large proportion (56%) of high shock stage (more than S4), whereas the ratio for H-chondrites is 14%.

(5) The difference between H and L groups is more striking at higher shock stages (S5-S6). 16% of L-chondrites were classified as S5, which is much higher than for H-chondrites (2%).

* Data from: http://tin.er.usgs.gov/meteor/metbull.php

Table 5 Comparison of shock stages between H and L group chondrites

	H										L					
	This work	Rate / %	Non-Antarctic	Rate / %	Feng	Rate / %	Stöffler	Rate / %	Summary	Rate / %	Feng	Rate / %	Stöffler	Rate / %	Summary	Rate / %
S1	5	11	4	16	4	10	2	6	15	10	2	4	1	4	3	4
S2	21	45	9	36	29	74	4	11	63	43	20	36	3	11	23	27
S3	12	26	10	40	5	13	22	63	49	34	12	21	8	29	20	24
S4	8	17	2	8	1	3	6	17	17	12	18	32	7	25	25	30
S5	1	2							1	1	4	7	6	21	10	12
S6							1	3	1	1			3	11	3	4

3.2 Petrology of shock veins in H-chondrites and constraints on their shock history

The shock veins in GRV H-chondrites are mostly thin, with the widest vein only about 250 μm in width. Thin shock veins should cool down much more quickly, therefore they can easily preserve high-pressure phases. However, except for GRV 022469, in which the high-pressure phase wadsleyite is found, the other GRV H-chondrites do not contain any high-pressure phases in their shock veins.

The coarse-grained porphyroclasts (>10 μm across) of shock veins in GRV H-chondrites are mainly composed of host-rock fragments and a lesser proportion of crystals from silicate melt, whereas the fine-grained matrix (<1–5 μm across) crystallized from silicate melt mainly consists of granular pyroxene, eutectic droplets of kamacite and troilite, and lesser amounts of other oxides. The mineral assemblage of the shock veins in the H-chondrites consists mostly of low-pressure phases, including olivine, low-Ca pyroxene, and small amounts of whitlockite and chromite. In contrast, the high-pressure phases, e.g., ringwoodite, majorite, and wadsleyite, usually occur in shock veins in L-chondrites[10, 15, 19]. Therefore, based on the mechanics of high-pressure phases[20–21], we suggest a scenario for the history of the H-chondrite parent body. Consider that the duration of a shock event in the H-chondrite parent body could be much shorter than that of an L-chondrite parent body, and the pressure could be released more quickly. As a result, the high-pressure phases should be more easily preserved. However, because the duration of high temperatures after the impact of shock event could be much longer than in the L-chondrite parent body, the high-pressure phases may have retro-metamorphosed and converted to the low-pressure minerals.

The fine-grained matrix of shock vein in GRV 053196 is composed of pyroxene (low-Ca pyroxene and diopside) and oxides crystallized from silicate melt, without majorite-pyrope being crystallized from the chondritic melt under high pressure, different from that of Yamato 751000 (H6, S6, by Tomioka et al.[22]) and other heavily shocked L-chondrites with matrices that contain a series of high-pressure minerals including a solid solution of majorite-pyrope or magnesiowüstite. GRV 053196, which does not contain any high-pressure features, is also different from Yamato 75267 (H6) in which both the high- and low-pressure regions were observed by Kimura[5]. The Fa and Fs values of olivine and pyroxene fragments in the GRV 053196 shock vein are slightly higher than those of the host olivine and pyroxene outside the shock vein, but their crystallographic structure didn't change. Based on the low-pressure assemblage of olivine and pyroxene in the shock vein, the shock pressure is estimated to have been less than 15 GPa[23].

3.3 Constraints on the shock history of ordinary chondrite parent bodies by shock vein assemblages

Wadsleyite is a polymorph of $(Mg,Fe)_2SiO_4$, the β-olivine, or an intermediate phase between olivine and ringwoodite. The structure of wadsleyite is similar to ringwoodite, but wadsleyite was not found during the conversion process of olivine to ringwoodite in high-pressure experiments[24]. The conversion of olivine to ringwoodite needs a great deal of energy, whereas the conversion of olivine to wadsleyite needs less energy. Based on the results of high-pressure experiments, wadsleyite may be formed during a shock event by first converting the olivine to ringwoodite then later transforming it into olivine. Whether ringwoodite will be transformed to wadsleyite or olivine depends on the amount of energy. Since the temperature is very high after H-chondrite is compacted, the high-pressure minerals are easier to convert into low-pressure minerals when the shock pressure was released.

In our study of H-chondrites from the Grove Mountains, only one meteorite, GRV 022469, was found to contain wadsleyite, which is surrounded by fine-grained pyroxene and oxides and shows no chemical zoning. These features suggest that the wadsleyite was converted through a solid state process. The wadsleyite in GRV 022469 could be formed by reverse transformation from ringwoodite. Based on the phase diagram of Allende[23], its shock peak pressure should be 15–18 GPa.

There are very few reports of high-pressure minerals

found in H-chondrites, except for Yanzhuang, Yamato 75100 and Yamato 75267. Two occurrences of ringwoodite, large fragments formed by solid-solid state transformation and fine-grained matrices crystallized from melt, have been found by Yanzhuang[8]. In Yamato 75100 and Yamato 75267, high-pressure phases, including ringwoodite, a solid-solution of majorite-pyrope, hollandite, and lesser amounts of akimotoite, are found. The ringwoodite was formed by solid-solid state transformation, whereas the majorite-pyrope solid solution formed by crystallization from melt[6– 7, 25–26]. In GRV 022469, the only high-pressure phase, wadsleyite, is also considered to be the result of solid-solid state transformation, but no other high-pressure phase that crystallized from melt was found.

No chemical zoning is found in the high-pressure phases of the four H-chondrites described above. In contrast, chemical zonation in the ringwoodite aggregates (Mg-rich in the core, Fe-rich in the rim) is obvious in Peace River (L6)[27]. The wadsleyite in GRV 022469 was transformed as a solid[28–29], which is similar to ringwoodite in Tenham (L6), but different from the high-pressure phases in Sixiangkou, which were formed by non-continuous crystallization[11]. The mineralogical and petrological features of these wadsleyite samples indicate that they are possibly transformed from olivine in solid-solid state under the high pressure caused by shock waves during impact events on the parent body.

4 Conclusions

(1) Based on shock metamorphic features, the shock stages of 47 GRV H-chondrites are classified as S1 (5), S2 (19), S3 (14), S4 (8) and S5 (1). Of the 47 H-chondrites from the Grove Mountains, GRV 022469 is the first H-chondrite in the Chinese Antarctic meteorite collection to be found with a high-pressure phase, and also only the fourth H-chondrite to be found anywhere on Earth with high-pressure phases.

(2) The shock stages of H-chondrites are lower, usually less than S4. H-chondrites from the Grove Mountains have a higher proportion of high shock stages (S4) than non-Antarctic meteorites, but have a lower proportion of high shock stages (higher than S4) than L-chondrites.

(3) The shock veins in H-chondrites are slightly narrower than those in L-chondrites. By comparing the mineral assemblages of these shock veins, a scenario for the general lack of high-pressure phases in H-chondrites is proposed. The duration of shock events in an H-chondrite parent body could be much shorter than in an L-chondrite parent body, resulting in a faster release of pressure and the easier preservation of high-pressure phases. However, the parent bodies of H-chondrites may have maintained high temperatures for a longer time after a shock event, so the high-pressure phases formed by solid transformation may be retro-metamorphosed to low-pressure ones, and its peak pressure is estimated to be less than 15 GPa.

(4) The wadsleyite observed in the shock vein in GRV 022469, combined with the mineralogy and petrology of high-pressure minerals found in other H-chondrites, indicates that wadsleyite in H-chondrites is formed by a shock-wave induced solid-state transformation resulting from a shock event in the H-chondrite parent body. This occurs during an intermediate process in the conversion of ringwoodite to olivine, with a peak pressure estimated to be around 15–18 GPa.

Acknowledgments This work is supported by the Pilot Project of Knowledge Innovation of Chinese Academy of Sciences (Grant no. KZCX2-YW-110) and the National Natural Science Foundation of China (Grant nos. 40673055 and 40473037) and the Open Foundation of Key Laboratory of Geological Engineering Centre of Guangxi Province (Grant no. Gui Ke Neng 07109011-K024).The authors would like to thank the Polar Research Institute of China for providing the research samples. We are also grateful to Prof. Wang Shijie, Vice-Prof. Liu Xiuming, Dr. Li Shijie, Assistant Prof. Qin Chaojian, and Xin Pushe for their great help with this work. In addition, we also appreciate the constructive suggestions of an anonymous reviewer and the assistance of Prof. Sha Liankun with English usage.

References

1 Sharp T G, P S DeCarli. Shock Effects in Meteorites, in Meteorites and the Early Solar System II, 2006: 653–677
2 Rubin A E. Chromite-Plagioclase assemblages as a new shock indicator: implications for the shock and thermal histories of ordinary chondrites. Geochimica et Cosmochimica Acta, 2003, 67(14): 2695–2709
3 Chen M, et al. Metal-troilite-magnetite assemblage in shock veins of Sixiangkou meteorite Geochimica et Cosmochimica Acta, 2002, 66(17): 3143–3149
4 Stöffler D, K Keil, E R D Scott. Shock metamorphism of ordinary chondrites. Geochimica et Cosmochimica Acta, 1991, 55: 3845–3867
5 Kimura M et al. Back-transformation of high-pressure phases in a shock melt vein of an H-chondrite during atmospheric passage: Implications for the survival of high-pressure phases after decompression. Earth and Planetary Science Letters, 2003, 217: 141–150
6 Kimura M, et al. Raman petrography of high-pressure minerals in H, L, LL and E-chondrites. Meteoritics and Planetary Science Supplement, 2001, 36: 99
7 Kimura M, et al. Natural Occurrence of High-Pressure Phases, Jadeite, Hollandite, Wadsleyite, and Majorite-Pyrope Garnet, in an H Chondrite, Yamato 75100. Meteoritics and Planetary Science Supplement, 2000, 35: 87
8 Chen M, Xie X D. The shock effects of olivine of Yanzhuan. Acta Mineralogica Sinica, 1993, 13(2): 109–114 (in Chinese with English Abstract)
9 Sharp T G, Chen M, A El Goresy. Mineralogy and microstructures of shock-induced melt veins in the Tenham (L6) chondrite. Lunar and Planetary Institute Science Conference Abstracts, 1997: 1283
10 Xie Z, T G Sharp. High-pressure phases in shock-induced melt veins of the Umbarger L6 chondrite: Constraints of shock pressure. Meteoritics & Planetary Science, 2004, 39: 2043–2054.
11 Chen M, et al. Fracture-related intracrystalline transformation of olivine to ringwoodite in the shocked Sixiangkou meteorite. Meteoritics and Planetary Science, 2006, 41: 731–737

12 Xie Z, T G. Sharp, and P. DeCarli: Pressure Histories from Thin and Thick Shock-induced Melt Veins in Meteorites. 36th Annual Lunar and Planetary Science Conference, 2005: 1216
13 Chen M, et al. A microstructural investigation of natural lamellar ringwoodite in olivine of the shocked Sixiangkou chondrite. Earth and Planetary Science Letters, 2007, 264: 277–283
14 Ohtani E, et al. Formation of high-pressure minerals in shocked L6 chondrite Yamato 791384: constraints on shock conditions and parent body size. Earth and Planetary Science Letters, 2004, 227: 505–515
15 Chen M, An El Goresy, P Gillet. Ringwoodite lamellae in olivine: Clues to olivine-ringwoodite phase transition mechanisms in shocked meteorites and subducting slabs. Proceedings of the National Academy of Science, 2004, 101: 15033–15037
16 Zhang A, et al. Assemblage of diopside, pyroxene, akimotoite, and ringwoodite in the heavily shocked Sixiangkou L6 chondrite: Further Constraints of Shock Metamorphism. 37th Annual Lunar and Planetary Science Conference, 2006: 1069
17 E l Goresy A, et al. Two distinct olivine-ringwoodite phase transition mechanisms in shocked L-chondrites: Genetic Implications. Meteoritics and Planetary Science Supplement, 2005, 40: 5010
18 Feng L, et al. Shock metamorphism of ordinary chondrites from Grove Mountains, Antarctica. Chinese Journal of Polar Science, 2009, 20: 187–199
19 Sharp T G, et al. Natural occurrence of MgSiO3-ilmenite and evidence for MgSiO3-perovskite in a shocked L chondrite. Science, 1997, 277: 352–355
20 Kerschhofer L, T G Sharp, D C Rubie. Intracrystalline transformation of olivine to Wadsleyite and Ringwoodite under subduction zone conditions. Science, 1996, 274: 79–81
21 Kerschhofer L, et al. Kinetics of intracrystalline olivine-ringwoodite transformation. Physics of the Earth and Planetary Interiors, 2000, 121: 59–76
22 Tomioka N, M Kimura. The breakdown of diopside to Ca-rich majorite and glass in a shocked H chondrite. Earth and Planetary Science Letters, 2003, 208: 271–278
23 Agee C B, et al. Pressure-temperature phase diagram for the Allende meteorite. Journal of Geophysical Research, 1995, 100: 17725–17740
24 Putnis A, G D Price. High-pressure (Mg, Fe)2SiO4 phases in the Tenham chondritic meteorite. Nature, 1979, 280: 217
25 Kimura M, et al. The first discovery of high-pressure polymorphs, jadeite, hollandite, wadsleyite and majorite, from an H-chondrite, Y-75100. Antarctic Meteorites XXV, 2000: 41–42
26 Kimura M, et al. Heavily shocked Antarctic H-chondrites: Petrology and shock history. Antarctic Meteorites XXIV, 1999: 67–68
27 El Goresy A, et al. Evidence for fractional crystallization of Wadsleyite and Ringwoodite from individual olivine melt pockets in chondrules entrained in shock melt veins. Meteoritics and Planetary Science Supplement, 2008, 43: 5002
28 Xie Z, T G Sharp. Host rock solid-state transformation in a shock-induced melt vein of Tenham L6 chondrite. Earth and Planetary Science Letters, 2007, 254: 433–445
29 Sharp T G, Z Xie, P S DeCarli. The Impact history of Chondrites as revealed by high-pressure minerals. AGU Fall Meeting Abstracts, 2005, 42: 3